

SPECTROSCOPIC SIGNATURES OF HALOGEN- π INTERACTION ON THE FLUORESCENCE OF BIPHENYL AND NAPHTHALENE ON Al_2O_3

Alan O. Lopez*, Caleb D. Tobey,* Brandon X. Moses* and A.M. Nishimura†

Department of Chemistry, Westmont College, Santa Barbara, CA 93108

Abstract

In order to investigate halogen- π interaction at the fundamental level, surface dynamics of vapor deposited fluorophores, naphthalene and biphenyl were observed by heating the substances that had been deposited on Al_2O_3 during a temperature programmed desorption (TPD) procedure. A series of dihalobutane s were deposited below the fluorophore: 1,4-difluorobutane, 1,4-dichlorobutane, 1,4-dibromobutane and 1,4-diiodobutane in separate experiments. For biphenyl, the ordering subsequent to the disorder-to-order transition was much more complete and the trap fluorescence was quenched. For naphthalene, the excimer that formed upon deposition was stabilized by the halogen bond that formed between the halogen and π -electrons that caused quenching by molecular aggregation.

†Corresponding author: nishimu@westmont.edu

*Undergraduate researchers and co-authors

Keywords: biphenyl, naphthalene, 1,4-dihalobutane, vapor deposition, fluorescence, halogen bond, halogen- π interaction, σ -hole

Submitted: July 10, 2025

Accepted: July 31, 2025

Revision received: August 22, 2025

Published: December 2, 2025

Introduction

In a recent study, biphenyl and naphthalene were used as a probe to characterize the surface morphology of the adlayers that they formed when 1-chloroalkanes and 1, ω -dichloroalkanes were vapor deposited on an Al_2O_3 surface.¹⁻⁴ Due to dispersion forces, the alkyl chains organized to form adsorption sites if the length of the alkyl moiety was sufficient to accommodate the fluorophore.^{5,6} In these cases,⁷⁻¹² the chlorine functional group forms a halogen-bond with the π -cloud of the fluorophore and causes nucleation-crystallization and fracturing of the ordered biphenyl molecules.¹⁻⁴ The result was enhanced fluorescence from the trap and the onset of the disorder-to-order transition in biphenyl.¹⁻⁴ For naphthalene, the stability of the excimer¹³ was emphasized in that the reportedly strong chlorine- π bond did not cause the onset of the excimer-to-order transition, except when the environmental thermal energy was just at the desorption of the haloalkane and naphthalene's excimer-to-order transition.^{3,4} A much higher fluorescence intensity of the ordered naphthalene was observed with the haloalkane underlayer than with neat naphthalene.^{3,4}

This study is a more systematic investigation into the halogen bond. Here, the hydrocarbon backbone was kept the same, i.e. with a 4-carbon chain, but the terminal halogens were varied. The strength of the halogen- π interaction in increasing order is $\text{F} < \text{Cl} < \text{Br} < \text{I}$, due to the increasing polarizability and the size of the σ -hole.⁷⁻¹⁰ Reported here is how the halogen bond affects the surface morphology of biphenyl and naphthalene by observing the spectral changes as the surface was heated. The aim of the study was to determine the spectroscopic signatures, if any, that will allow the identification of the halogen bond during the TPD of these two fluorophores on Al_2O_3 .

Experimental

Biphenyl, naphthalene, 1,4-difluorobutane, 1,4-dichlorobutane, 1,4-dibromobutane, 1,4-diiodobutane were of the highest purity (> 99%) that could be purchased from commercial sources (Sigma-Aldrich, St. Louis, MO). The details of the experimental set-up were described in detail in the previous papers¹⁻⁴ and are summarized here. These compounds were placed in a sample holder attached to one end of a precision leak valve for vapor deposition that led into the main ultra-high vacuum chamber. The substrate

was a single crystal of Al_2O_3 (0001) that was suspended on the lower end of a liquid nitrogen cryostat.

The fluorophores were optically pumped with a high pressure mercury lamp and the wavelength selected at 250 nm with a 0.25 m monochromator. Resistive heating of the Al_2O_3 was done by sending current through a thin tantalum foil that was in thermal contact with the substrate. A process controlling code was written in LabVIEW that monitored the surface temperature via a thermocouple that was also in contact with the Al_2O_3 and via a feedback program, controlled the current. The temperature ramp for the TPD was linear to $1.98 \pm 0.01 \text{ K s}^{-1}$. During the TPD, the program also took the fluorescence spectra every 300 ms in real time using a spectrometer with input connected to a fiber-optic cable that fed into the chamber. A lens was mounted on the end to collect the fluorescence.

To ensure a clean surface, the Al_2O_3 was heated to 300 K after each run. Temperature ramps to higher temperatures did not indicate any other adsorbates.¹⁻⁴

The activation energy for desorption, E_a , was calculated by Redhead analysis in which a first-order desorption kinetics, as described by King, was assumed and is based on the mass spectral peak desorption temperature, T_p .¹⁴⁻¹⁶ The uncertainties in the desorption temperatures lead to a propagated error in the activation energies of $\pm 2\%$, unless otherwise stated.

The LabVIEW coded program also received data from a residual gas analyzer so that both the deposition and the desorption of biphenyl, naphthalene and the other adsorbates could be monitored. The surface coverages, Θ , in monolayers (ML) were calculated by calibrating the integrated mass spectral peaks via an optical interference experiment.^{17,18} The interference experiment yielded accurate rate of deposition with coverage error of $\pm 30\%$, and is described in detail elsewhere.¹⁸

Transmittance of the excitation light at 250 nm was detected with a photomultiplier whose output was connected to a computer interfaced high resolution analog-to-digital converter that the same LabVIEW program controlled.

A pulsed quadrupled Nd:YAG laser with output at 266 nm

was the excitation source for the laser-induced fluorescence, LIF, measurements. The fluorescence was focused with a short focal length lens onto a 0.25 m monochromator equipped with a photomultiplier. The LIF was assumed to decay by first-order kinetics. A least square curve-fitting program was used to determine the slopes of this line, i.e. the rate constants, in real-time during the TPD experiment.

Results and Discussion

Biphenyl

Shown in Figure 1 is a wavelength-resolved TPD of a biphenyl multilayer (neat, single adsorbate). The arrangement of biphenyl molecules in the vapor deposited adlayer that is known to be amorphous and disordered with a λ_{max} at 318 nm.¹⁻⁴ At 160 K during the TPD, the adlayer underwent a transition from disorder to a more ordered arrangement that is characterized by the λ_{max} red-shift to 338 nm. This can be seen in Figure 1. In this ordered arrangement, resonant energy transfer pathway competes with the radiative relaxation and quenches the fluorescence to ~10 % of the initial intensity. The peak desorption temperature, T_p , of neat biphenyl at low coverages was 229 K. First-order desorption was assumed and the activation energy for desorption, E_a , was calculated to be 60 kJ/mol¹⁴⁻¹⁶ and is listed in Table 1 with T_p 's and E_a 's of all the other compounds in this study.

1,4-Difluorobutane/biphenyl

Shown in Figure 2 is the wavelength-resolved TPD of a bilayer composed of 1,4-difluorobutane and biphenyl. 1,4-difluorobutane was the underlayer and biphenyl was dosed on top. The disorder-

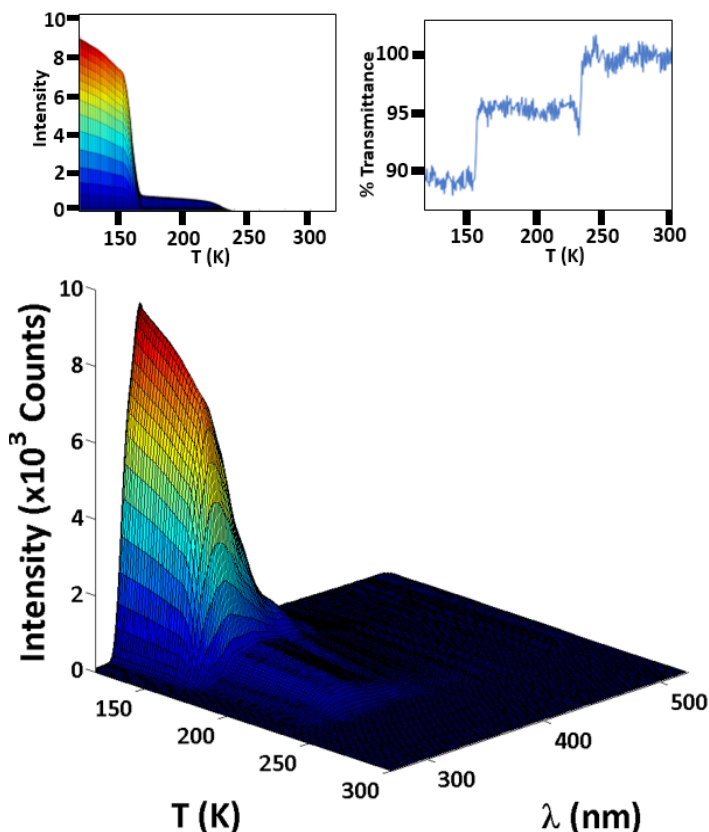


Figure 1. Wavelength-resolved TPD of biphenyl with a λ_{max} at 318 nm. The disorder-to-order transition occurred at about 160 K and λ_{max} red-shifted to 338 nm. $\Theta_{\text{biphenyl}} \sim 89$ ML. Left and right inset: side view and % transmittance, respectively.

to-order transition occurred with a very rapid decrease in the fluorescence intensity of the trap (Cf. left inset). The transmittance showed the rise in the transmittance simultaneously to the disorder-to-order transition. Aggregation-caused quenching is postulated because the transmittance as seen in the right inset is lower by about 20% compared to multilayer biphenyl.

1,4-Dichlorobutane/biphenyl

Shown in Figure 3 is the wavelength-resolved TPD of bilayer composed of 1,4-dichlorobutane as the underlayer and biphenyl. Three observations can be made. First the disorder-to-order transition begins at about 145 K, which is about 15 K lower than for the multilayer biphenyl. Second, the fluorescence intensity after the red-shift that is the spectroscopic signature for the disorder-to-order transition remains high, relative to the multilayer spectra. Higher intensity after the transition has been attributed to the increase in the density of trap that was caused by the presence of 1,4-dichlorobutane. The underlayer desorbs at 188 K, and was coincident with the maximum in the fluorescence intensity. It is interesting to note that the minimum in the transmittance occurred at about 225 K, which is optically about half way down the decreasing part of the wavelength-resolved TPD.

1,4-Dibromobutane/biphenyl

Shown in Figure 4 is the wavelength-resolved TPD of a bilayer of 1,4-dibromobutane and biphenyl. Three observations are again noted. First as was the case for 1,4-dichlorobutane underlayer, the onset of the disorder-to-order transition in biphenyl occurred about 15 K below that of the multilayer. Second, the quenching of the fluorescence due to energy transfer at 155 K is more than that for the multilayer. Finally subsequent to the disorder-to-order transition the increase in the trap fluorescence reached a maximum that

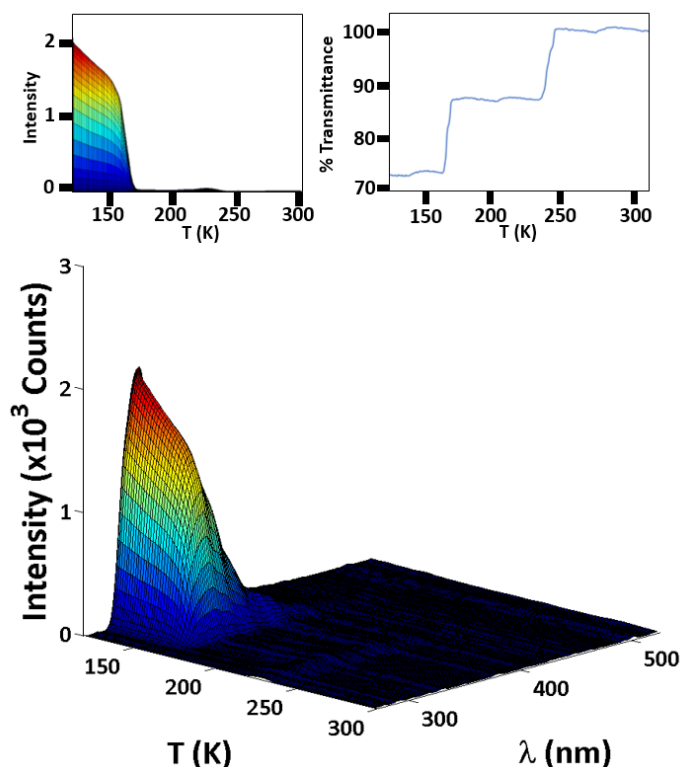


Figure 2. 1,4-difluorobutane/biphenyl bilayer with $\Theta_{1,4\text{-difluorobutane}} \sim 100$ ML and $\Theta_{\text{bi-phenyl}} \sim 100$ ML. The underlayer was annealed at 160 K 30 seconds prior to the deposition of biphenyl. Insets: left is the intensity versus temperature, side view. On the right is the transmittance of the 250 nm excitation light.

coincided with the desorption of the underlayer. This is due to the percolation and passage of the underlayer through the biphenyl layer.

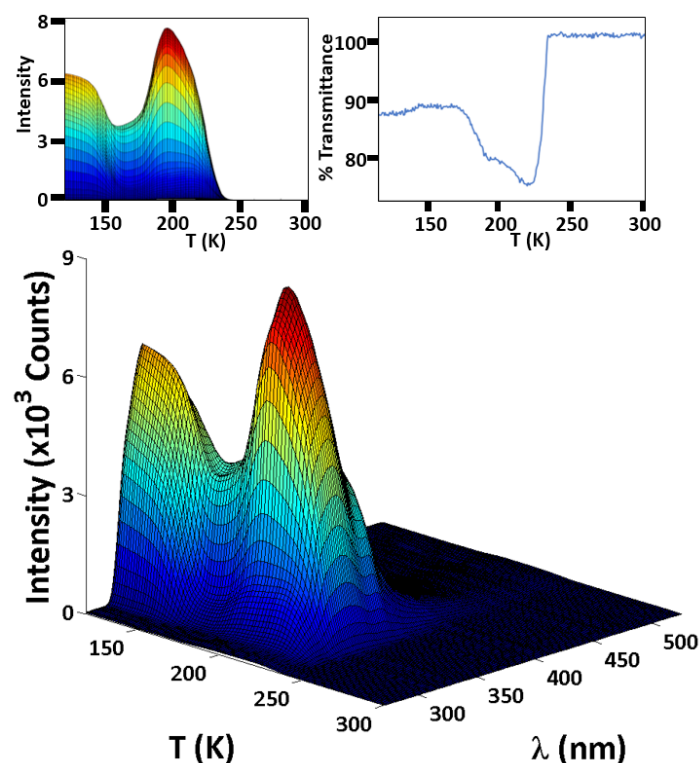


Figure 3. 1,4-dichlorobutane/biphenyl bilayer with $\Theta_{1,4\text{-dichlorobutane}} = 79$ ML and $\Theta_{\text{biphenyl}} = 90$ ML. The underlayer was annealed at 170 K for 30 seconds prior to the deposition of biphenyl. Insets: left is the intensity versus temperature, side view. On the right is the transmittance of the 250 nm excitation light.

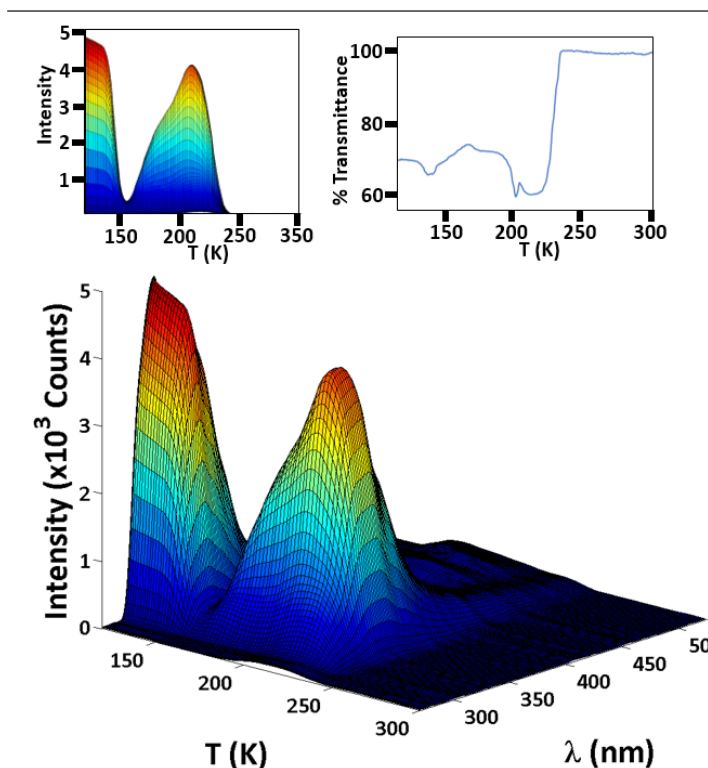


Figure 4. 1,4-dibromobutane/biphenyl bilayer with $\Theta_{1,4\text{-dibromobutane}} = 247$ ML and $\Theta_{\text{biphenyl}} = 98$ ML. The underlayer was not annealed prior to the deposition of biphenyl. Insets: left is the intensity versus temperature. On the right is the transmittance of the 250 nm excitation light during the TPD.

The transmittance varies little during the TPD. However, at the minimum in the fluorescence, there is a slight decrease in the transmittance, and a sharp decrease due to scattering is observed at the temperature at which the 1,4-dibromobutane desorbed.^{3,4}

1,4-Diiodobutane/biphenyl

Shown in Figure 5 is the wavelength-resolved TPD of a bilayer of 1,4-diiodobutane and biphenyl. The onset and the completion of the disorder-to-order transition was similar to that for the multilayer biphenyl. However the huge difference here compared to the multilayer was the observed degree to which quenching occurred due to energy transfer, down to about 3% of the initial intensity. Then just as 1,4-diiodobutane desorbed at 222 ± 2 K (Cf. Table 1), the fluorescence intensity of the trap with well-resolved vibrational progression increased to about 26% of the original intensity.

The transmittance exhibited the characteristic rise at the disorder-to-order transition. Due to scattering, the dip in transmittance occurred as the 1,4-diiodobutane desorbed. During the TPD, there was an overall quenching of the fluorescence by about 50% relative to multilayer biphenyl.

Display of halogen- π interaction on biphenyl fluorescence

As the dihalobutane moved through the biphenyl adlayer, the spectroscopic signatures of the effect that the halogen bond has on biphenyl on are: first the ordered form of biphenyl subsequent to the disorder-to-order transition was the most apparent. This is manifest in the progressively lower intensity of the fluorescence with a concomitant low transmittance. This is indicative of a higher degree of energy transfer and consequently, ordering, than found in multilayer biphenyl. Second the halobutanes serve to fracture

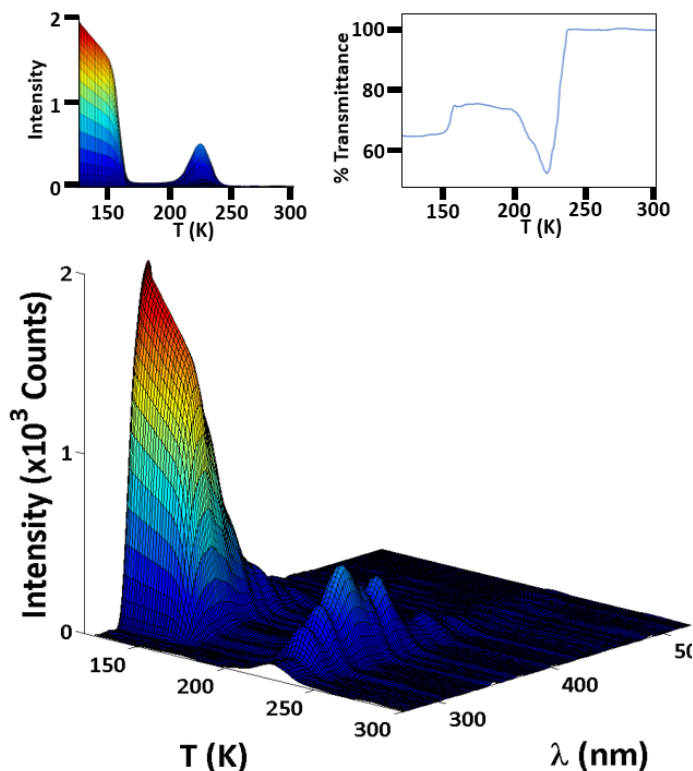


Figure 5. 1,4-diiodobutane/biphenyl bilayer with $\Theta_{1,4\text{-diiodobutane}} = 265$ ML and $\Theta_{\text{biphenyl}} = 87$ ML. The underlayer was not annealed prior to the deposition of biphenyl. Insets: left is the intensity versus temperature. On the right is the transmittance of the 250 nm excitation light.

the aggregates of ordered biphenyl clusters subsequent to the disorder-to-order transition. This is evidenced by the increase in the biphenyl trap fluorescence, particularly with the 1,4-dichlorobutane and 1,4-dibromobutane. Finally, the 1,4-diiodobutane causes a high degree of ordering, almost crystal-like, as depicted by the resolved vibronic structure as the underlayer moved through the biphenyl adlayer.

Naphthalene

Shown in Figure 6 is the wavelength-resolved TPD of naphthalene. The adlayer that formed when naphthalene is vapor deposited on Al_2O_3 was amorphous and optical pumping exhibited excimer fluorescence.^{13,19} During the TPD, the adsorbate transitioned from the amorphous morphology to a more ordered state just prior to desorption.¹⁹ The measured transmittance (Cf. right inset) did not fall below about 4% with a signal-to-noise ratio of of 1:1. The fluorescence intensity was relatively high even with very low absorption of the excitation light. This would be indicative of very high quantum yield for the naphthalene excimer.

The left inset in Figure 6 shows the LIF rate constant to increase monotonically from about 8×10^6 to $9 \times 10^6 \text{ s}^{-1}$. The increase was attributed to thermally induced quenching, as can be seen from decreasing intensity of the excimer fluorescence. The lifetimes, which are the inverse of the rate constants, were consistent with those previously reported.¹³

1,4-Difluorobutane/naphthalene

Shown in Figure 7 is the wavelength-resolved TPD of bilayer of 1,4-difluorobutane and naphthalene. What is immediately apparent is that the overall intensity was decreased by about 30% (note the change in the vertical axis scale) and is attributed to aggregation-caused quenching due to halogen- π interaction. The

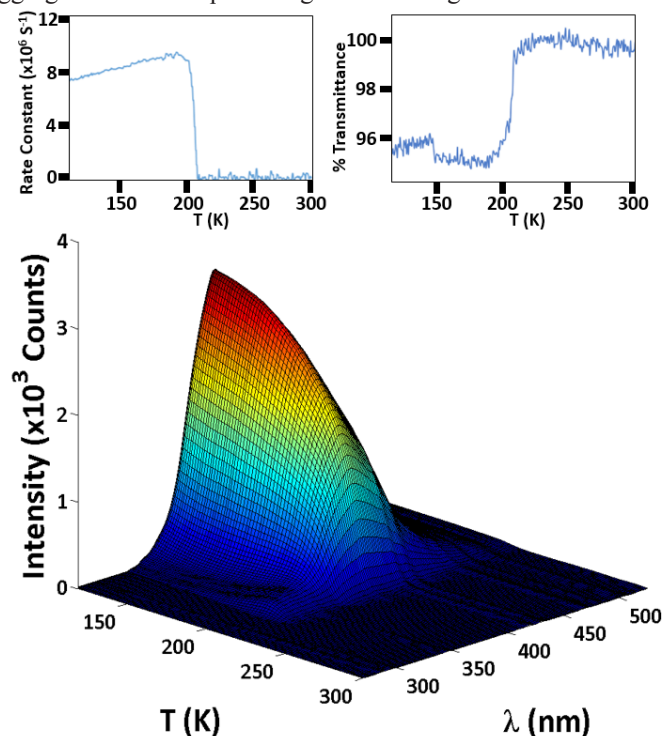


Figure 6. Wavelength-resolved TPD of naphthalene neat with coverage of 92 ML. The excimer has a $\lambda_{\text{max}} = 398 \text{ nm}$. The excimer-to-order transition occurs at 200 K during the TPD, but the trap emission from the ordered state is barely visible. Right inset: % transmittance vs. T during the TPD. Left inset: LIF rate constants vs T during the TPD.

excimer-to-order transition was not detected. The LIF decay rate constant was not affected. The lower % transmittance (Cf. right inset) supports the postulate that aggregation-caused quenching was the cause of the lower fluorescence intensity.

1,4-Dichlorobutane/naphthalene

Shown in Figure 8 is the wavelength-resolved TPD of a bilayer of 1,4-dichlorobutane and naphthalene. The excimer intensity was enhanced as the 1,4-dichlorobutane percolated and passed through the naphthalene. As it did so, the rate constant decreased momentarily during the TPD experiment. This has been postulated to be due to the separation of the fluorophoric molecules due to the passage of the 1,4-dichlorobutane. Simultaneously the transmittance decreased as was observed in the previous bilayers with naphthalene.

1,4-Dibromobutane/naphthalene

Shown in Figure 9 is the wavelength-resolved TPD of a bilayer of 1,4-dibromobutane and naphthalene. When comparing the effect of 1,4-dichlorobutane as an underlayer with 1,4-dibromobutane (Cf. Figures 8 and 9), it was observed that, with the 1,4-dichlorobutane, the excimer intensity was enhanced, whereas with 1,4-dibromobutane, the underlayer served to induce the excimer-to-order transition. It should be noted that the desorption of 1,4-dibromobutane occurred within 5 K of naphthalene's desorption temperature (Cf. Table 1), and the excimer-to-order transition might be concerted with what would occur with neat naphthalene. Also unique to 1,4-dichloro- and 1,4-dibromobutane was that the LIF decay rate constants were lower than for the neat naphthalene and for the bilayer with the other 1,4-dihaloalkanes.

1,4-Diiodobutane/naphthalene

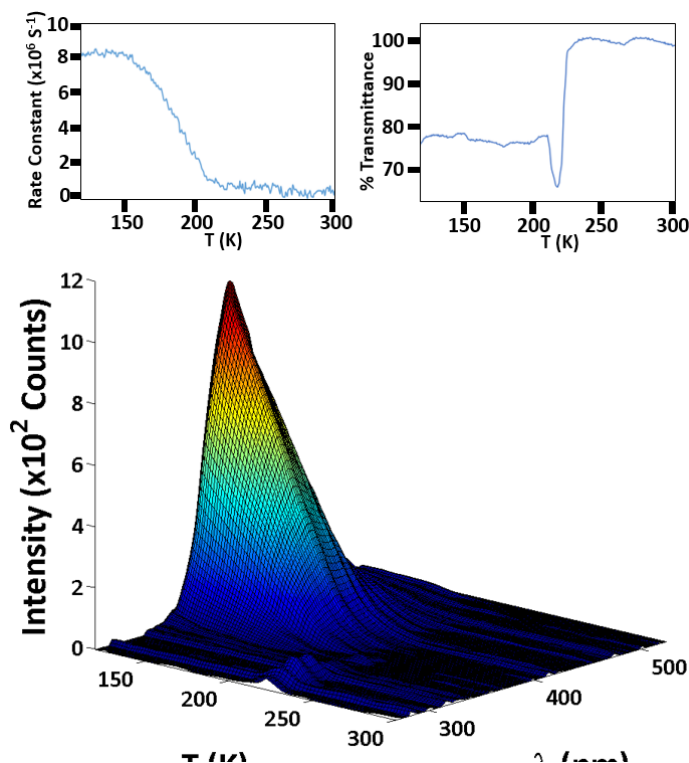


Figure 7. Wavelength-resolved TPD of naphthalene with $\Theta_{\text{naphthalene}} \sim 100 \text{ ML}$ with an underlayer of 1,4-difluorobutane with $\sim \Theta_{\text{1,4-difluorobutane}} \sim 100 \text{ ML}$ that had not been annealed. Left inset: LIF rate constants vs. T during the TPD. Right inset: % transmittance vs T during the TPD.

Shown in Figure 10 is the wavelength-resolved TPD of a bilayer composed of 1,4-diiodobutane with naphthalene as the upper layer. After deposition, the intensity of the naphthalene fluorescence is much lower than for the multilayer. Quenching of

the excimer fluorescence persisted throughout the TPD, and the excimer-to-order transition is barely visible.

Effect of halogen- π interaction on naphthalene excimer fluorescence

A general trend that depicts the progressive degree of halogen- π interaction with $F < Cl < Br < I$ is more difficult to identify for the naphthalene excimer fluorescence. The 1,4-difluorobutane and 1,4-diiodobutane gave rise to a very similar effect on the naphthalene excimer. Thermal quenching resulted in an almost linear decrease in the excimer intensity profile during the TPD. With both underlayers, the excimer-to-order transition was barely detectable. This has been tentatively attributed to the stabilization of the excimer by the dihalobutanes via halogen- π interaction. That is, these two underlayers served to hold the morphology of the adlayer in place so that the excimer persisted through desorption.

As desorption occurred for bilayers containing 1,4-dichlorobutane and 1,4-dibromobutane, the passage, particularly of 1,4-dichlorobutane caused the separation of the molecules involved in the formation of excimers, and thereby reducing aggregation-caused quenching. In addition, these two underlayers induced the excimer-to-trap transition. This was evidenced by the trap fluorescence that was clearly observed. Overall spectroscopic signatures were not as dramatic when compared to the effect alkanes alone have on the excimer fluorescence of naphthalene.¹⁹ This might be expected since the halogen- π interaction could be postulated to stabilize the excimer which held the naphthalene in that state from deposition to desorption.

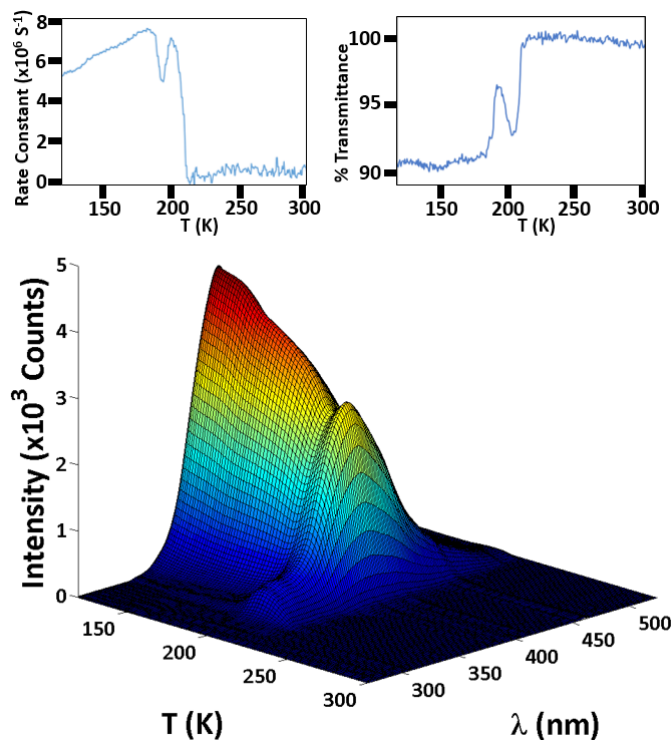


Figure 8. Wavelength-resolved TPD of naphthalene with $\Theta_{\text{naphthalene}} = 84$ ML with an underlayer of 1,4-dichlorobutane with $\Theta_{\text{1,4-dichlorobutane}} = 141$ ML that had been annealed at 130 K for 30 s. Left inset: LIF rate constants vs. T during the TPD. Right inset: % transmittance vs T during the TPD.

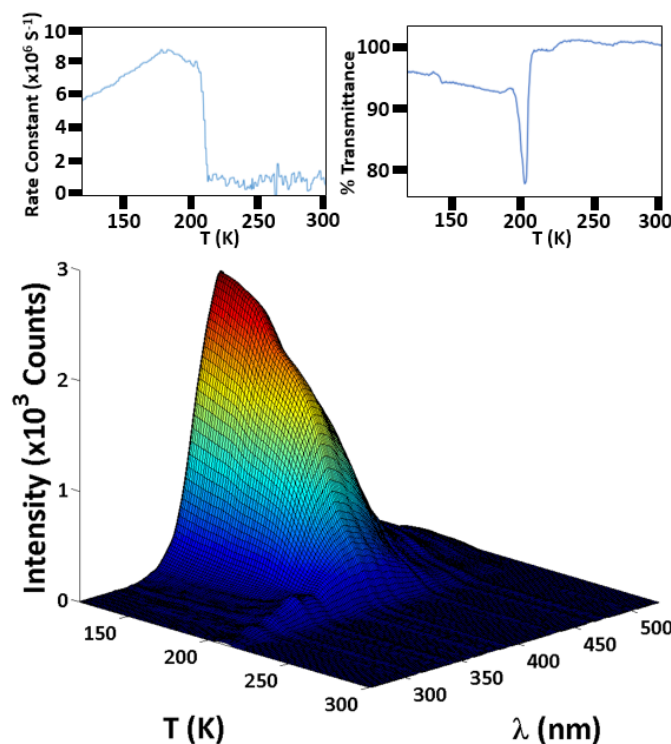


Figure 9. Wavelength resolved TPD of 1,4-dibromobutane/naphthalene bilayer with $\Theta_{\text{1,4-dibromobutane}} = 134$ ML and $\Theta_{\text{naphthalene}} = 80$ ML. Left and right insets are the LIF rate constants and % transmittance as a function of temperature during the TPD, respectively.

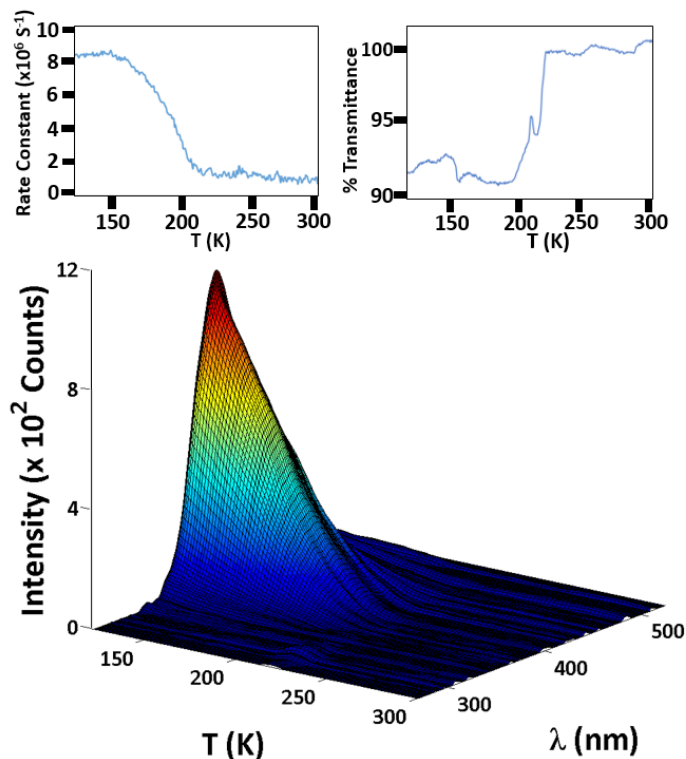


Figure 10. Wavelength resolved TPD of 1,4-diiodobutane/naphthalene bilayer with $\Theta_{\text{1,4-diiodobutane}} = 154$ ML and $\Theta_{\text{naphthalene}} = 80$ ML. Right and left insets are the % transmittance and the LIF rate constants as a function of temperature during the TPD, respectively.

Acknowledgment

The authors would like to thank the John Stauffer Charitable Trust for funding the student stipends for summer research. This work was supported by the donors of ACS Petroleum Research Fund under Undergraduate Research #68385-UR5 and -S24.

Table 1. Desorption activation energies, E_a 's, in kJ/mol for all of the compounds in this study as calculated from their respective T_p 's in K.¹⁴⁻¹⁶

	T_p (K)	E_a (kJ/mol)
1,4-difluorobutane	218 ± 1	56.5 ± 0.3
1,4-dichlorobutane	184 ± 4	47 ± 1
1,4-dibromobutane	203 ± 2	52 ± 0.5
1,4-diiodobutane	222 ± 2	57.5 ± 0.6
biphenyl	231 ± 1	60.0 ± 0.3
naphthalene	211 ± 1	54.7 ± 0.2

References

1. A.O. Lopez, J.C. Nieman, J.M. Rosenfeld, R.M. Toepfer and A.M. Nishimura, *JUCR*, **2024**, 23, 31-38.
2. J.M. Rosenfeld, R.M. Toepfer, A.O. Lopez, J.C. Nieman, I. Felix, J. Zerwas and A.M. Nishimura, *JUCR*, **2024**, 23, 25-30.
3. Alan O. Lopez, Brandon X. Moses, Caleb D. Tobey, Johnathan Arrieta, Mason Ticas, Jackson Zerwas and A.M. Nishimura, *JUCR*, **2025**, 24, 59-65/
4. Brandon X. Moses, Caleb D. Tobey, Alan O. Lopez and A.M. Nishimura, *JUCR*, **2025**, 24, 66-72.
5. M. Frederick, J. Fowkes, *J. Phys. Chem.*, **1980**, 84, 510-512.
6. M. Anwar, F. Turci and T. Schilling, *J. Chem. Phys.* **2013**, 139, 214904.
7. T. Arnold, C.C. Dong, R.K. Thomas, M.A. Castro, A. Perdigon, S.M. Clarke and A. Inaba, *Phys. Chem. Chem. Phys.*, **2002**, 4, 3430-3435.
8. T. Arnold, R.K. Thomas, M.A. Castro, S.M. Clarke, L. Messe and A. Inaba, *Phys. Chem. Chem. Phys.*, **2002**, 4, 345-351.
9. K.E. Riley and K.A. Tran, *Crystals*, **2017**, 7, <https://doi.org/10.3390/cryst7090273>.
10. K. Shimizu and J.F. da Silva, *Molecules*, **2018**, 23 2959. <https://doi.org/10.3390/molecules23112959>
11. M.M. Popa, D.E. Dumitrescu, S. Shova and I. C. Man, *Crystals*, **2020**, 10, 1149, DOI: 10.3390/cryst10121149. 5-Iodo-1-Arylpzrazoles as benchmarks for invstigating the tuning of the halogen bond.
12. H.G. Wallnoefer, T. Fox, K.R. Liedl and C.S. Tautermann, *Phys. Chem. Chem. Phys.* **2010**, 12, 14941-14949; DOI: 10.1039/CoCP00607F. dispersion dominated halogen-pi interactions: energies and location of minima calculations
13. J.B. Birks. *Photophysics of Aromatic Molecules*, John Wiley & Sons Ltd., New York, NY (1970), pp. 301-370.
14. P.A. Redhead. *Vacuum*, **1962**, 12, 203-211.
15. F.M. Lord and J.S. Kittelberger. *Surf. Sci.*, **1974**, 43, 173-182.
16. D.A. King. *Surf. Sci.*, **1975**, 47, 384-402.
17. S.A. Riley, N.R. Franklin, B. Ourdinarath, S. Wong, D. Congalton, and A.M. Nishimura, *J. Chem. Edu.* **1997**, 74, 1320-1322.
18. M.K. Condie, B.D. Fonda, Z.E. Moreau and A.M. Nishimura, *Thin Solid Films*, **2020**, 697, 137823-137828.

19. A.M. Nishimura, B.D. Fonda, J.B. Cleek and K.A. Martin, *JUCR*, **2017**, 16, 85-88.